NANO LETTERS

LETTER

pubs.acs.org/NanoLett

Photoinduced Ordering of Block Copolymers

Vikram K. Daga,[†] Evan L. Schwartz,[§] Curran M. Chandler,[‡] Jin-Kyun Lee,[∥,§] Ying Lin,[‡] Christopher K. Ober,[§] and James J. Watkins*[,‡]

[†]Department of Chemical Engineering and [‡]Polymer Science and Engineering Department, University of Massachusetts, Amherst, Massachusetts 01003, United States

[§]Department of Materials Science and Engineering, Cornell University, Ithaca, New York 14853, United States

Supporting Information

ABSTRACT: Photoinduced ordering of disordered block copolymers (BCPs) would provide an on-demand, nonintrusive route for formation of well-ordered nanostructures in arbitrarily defined regions of an otherwise disordered material. Here we achieve this objective using a rapid and simple approach in which photoconversion of an additive blended with the BCP introduces strong interactions between the additive and one of the chain segments and induces strong order in the BCP blend. The strategy is generally applicable to block copolymers containing chain segments capable of hydrogen bonding with the additive.

KEYWORDS: Block copolymer, photoinduced ordering, disorder-to-order transition, self-assembly

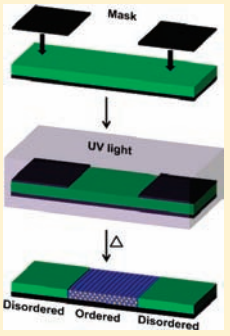

Block copolymers (BCPs) exhibit great promise as nanostructured materials and templates because of their ability to spontaneously self-assemble to form well-ordered periodic morphologies with typical domain sizes on the order of 10−50 nm. For BCP thin films, many techniques have been devised to manipulate and improve domain order and domain alignment.[1,2] These include chemical[3−5] or topographical[6,7] modification of substrates as well as processing methods that include solvent annealing and controlled evaporation of solvent,[8−11] use of neutral surfaces,[5,12] or treatment with electric fields.[13] The resulting well-ordered films find utility in device fabrication,[14−17] including their use as lithographic masks or masters for ultrahigh density magnetic storage media[6,7,18] or as templates in fabrication of inorganic mesostructured materials[19−21] and polymeric nanoporous membranes.[22,23] Here, we describe the design of novel BCP-additive systems which transition from a disordered state to a well-ordered state via a simple, on-demand photoinduced ordering process. Moreover, a photomask can be employed for carrying out photoinduced ordering in a region-selective manner such that only the regions that are exposed to light become ordered while the rest of the film does not show formation of ordered block copolymer morphology. This strategy provides a straightforward, nonintrusive means to form well-ordered chemical and topographical patterns within arbitrary regions of the target surface. Region-selective nanoscale pattern generation will offer new opportunities for device fabrication. These include the preparation of underlayers for ordering of another block copolymer film or liquid crystal layer and etch masks for subtractive processing of nanopatterned surfaces for use in applications such as nanofluidics and sensors. In the example provided here, the nanostructures formed in the exposed regions bear carboxylic acid groups in one of the domains of the block copolymer structure while the other domain is free of any reactive functionality. The carboxylic acid groups can be used to tether other functional materials such as nanowires,[24,25] biomacromolecules, or polymer brushes in a region-selective manner[26] for use in sensors and other nanoscale devices.

A−B and A−B−A type BCPs can form spherical, cylindrical, and lamellar domains arranged on periodic lattices[27] in which the morphology is determined mainly by the volume fraction of A and B phases. When the critical segregation strength required for microphase separation is not met, the blocks of a BCP do not phase segregate and the BCP remains disordered. The segregation strength is determined by the product of the Flory interaction parameter χ and N, the number of repeat units within the copolymer. Therefore, the product χN sets the lower limit for the formation of an ordered morphology and for the domain spacing and domain size, which scale with N for a given BCP. Incorporation of certain selectively interacting additives in disordered BCPs has been shown to enhance the segregation of the different blocks and thus lead to ordering and access to smaller domain spacing and sizes. For example, Bates and co-workers[28,29] and Russell and co-workers[7,30] have demonstrated examples in which addition of complexing salts to PEO containing disordered BCPs resulted in ordering. Similarly Watkins and co-workers demonstrated that the addition of homopolymers that selectively associate through hydrogen bonding with the poly(ethylene oxide) blocks of disordered Pluronic triblock copolymer surfactants (PEO−PPO−PEO, PEO = poly(ethylene oxide),

Received: November 23, 2010
Revised: January 24, 2011
Published: January 31, 2011

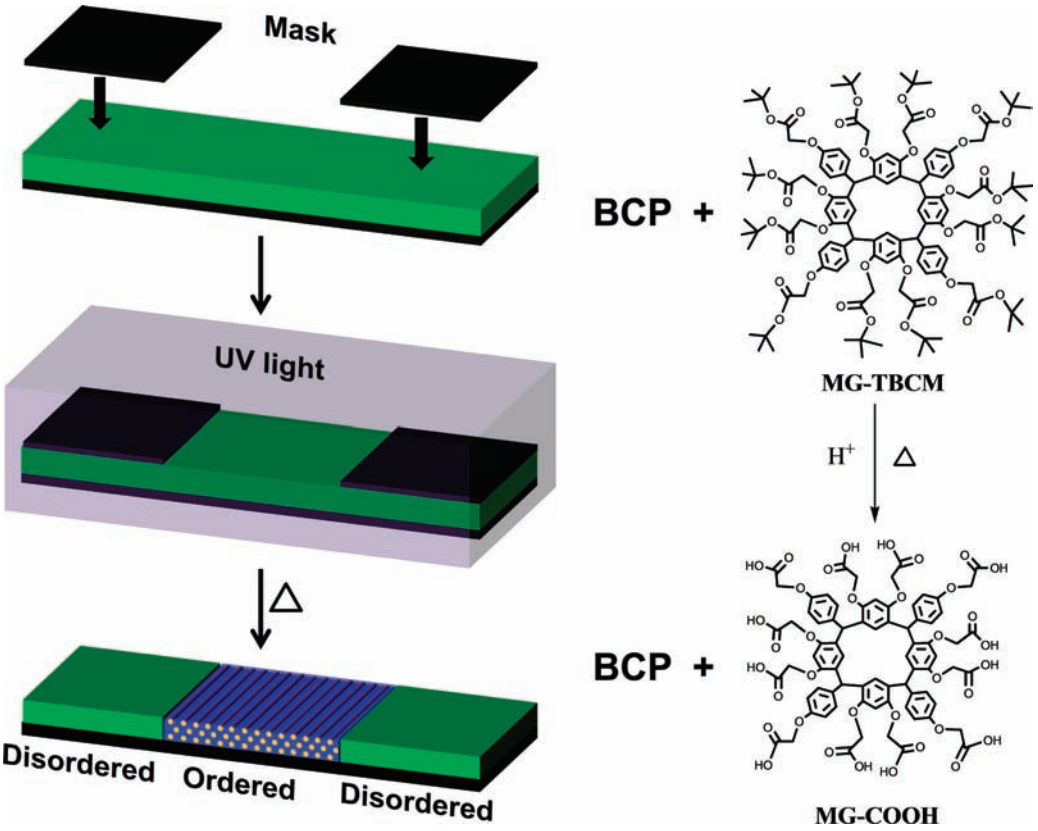

Figure 1. Schematic representation of the photoinduced ordering process (left) and the underlying reaction (right). Upon spin coating a blend of F127, MG-TBCM, and a photoacid generator, the film is disordered (green). Upon irradiation of the disordered film with UV light through a mask placed on top, a photogenerated acid is liberated in the exposed regions, which drives the chemical transformation of MG-TBCM to MG-COOH (reaction on right) upon baking while the unexposed regions remain unchanged. MG-COOH interacts strongly via hydrogen bonding with PEO resulting in spontaneous formation of microstructure due to disorder-to-order transition of F127 as PPO microphase separates as cylinders (orange) from the PEO + MG-COOH + photoacid phase which form the matrix (blue).

PPO = poly(propylene oxide)) induces microphase segregation and strong order.[31,32] The enhanced propensity of the blocks to phase segregate upon addition of additives is due to selective favorable interaction of the additive with the incorporating block. We recently made progress in elaborating the additive molecular design that leads to a disorder-to-order transition (DOT) and found that small molecule additives, including single and multiring aromatic cores[33] and polyhedral oligomeric silsesquioxanes functionalized with multiple hydrogen bonding sites at their periphery, can likewise induce order in Pluronic surfactants and other PEO containing block copolymers. We note that it is advantageous to use Pluronic block copolymer surfactants, as these are available at a commodity scale and thus are ideal for targeting low cost, high volume applications of BCP templates.

In all the above additive-driven assembly approaches, the chemical identity of the additives was preprogrammed to facilitate selective interaction with one of the blocks, thereby enhancing the segregation strength between the blocks and induce ordering. We introduce a new paradigm in the design of additive-loaded BCP systems. Here the blends of additive and BCP are initially disordered but can undergo a DOT upon chemical transformation of the additive induced by an external trigger, such as moderate heating in the presence of a catalytic amount of a third component (an organic acid) or photogeneration of the catalyst followed by moderate heating. This requires a design in which the additive initially exhibits compatibility, but weak interaction with the copolymer and in which in situ transformation of the additive induces sufficiently strong preferential interactions with one of the blocks as to induce order. Here we choose acid catalyzed deprotection of the additive functional groups to modulate their interaction with the copolymer host. After establishing that these systems undergo a DOT upon additive deprotection, the organic acid catalyst is replaced with a photoacid generator (PAG) to allow creation of acid in light-exposed regions only. Thus, coupled with the use of a photomask, the photoinduced ordering process enables region-selective control of the DOT in the copolymer film as shown schematically in Figure 1. Figure 1 also shows the additive employed in its protected and deprotected forms. We refer to the protected form of the additive as MG-TBCM as it belongs to the family of molecular glasses (MGs) based on a calix[4] resorcinarene structure and is protected with *tert*-butoxycarbonylmethyl (TBCM) groups. Upon baking at moderate temperature in the presence of a strong acid, the TBCM protecting group easily deprotects to form carboxylic acid groups resulting in formation of deprotected MG (i.e., MG-COOH).[34]

Photoresponsiveness has previously been imparted to polymers by chemically grafting photosensitive moieties on their chains. These moieties undergo chemical or isomeric transformations when exposed to light of certain wavelengths. In many instances, the trans−cis and cis−trans isomerization of azobenzene groups upon exposure to UV light at wavelengths 352 and

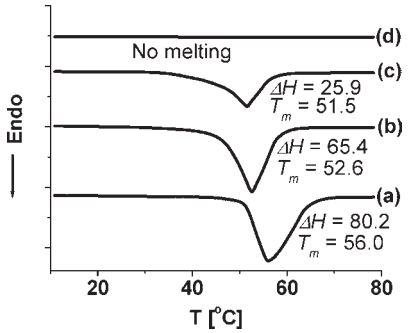

Figure 2. DSC thermograms of (a) neat F127, (b) 5/95 blend of PTSA/F127, (c) 40/60 blend of MG-TBCM/F127, and (d) 40/60/5 blend of MG-TBCM/F127/PTSA (MG-TBCM here is actually converted to MG-COOH). The thermograms have been shifted vertically to avoid overlap. The melting temperature (°C) and melting enthalpy *J*/(g of PEO) are mentioned beside each curve where melting was seen.

419 nm, respectively, have been employed to enable such transformations. For example, exposure to light was shown to influence the orientation of the domains of BCPs with azobenzene moieties grafted on one of its blocks.[35−38] In other work, UV induced photodimerization of anthracene has also been employed to control micrometer scale morphology of homopolymer blends.[39] A recent review describes the behavior of block copolymer systems with photosensitive moieties grafted on them.[40] Several examples of photoinduced transitions exist for such block copolymers in solution form, for example, photoinduced sol−gel transitions.[41] In bulk form, such modified block copolymers have been shown to be affected by light and various studies have been performed on various microphase separated block copolymers to study the effect of exposure to light on morphological transitions. For instance, Xu and co-workers showed how the arrangement of nanoparticles in an ordered BCP is affected by such transitions.[42] In all these cases the block copolymers were already structured and light was used to tailor that structure, for example, alter the domain orientation or enhance their alignment. Here, we focus on the formation of structure by inducing a DOT in an otherwise disordered block copolymer system.

However, attempts to cause a photoinduced DOT of such modified BCPs have not yet been very successful in demonstrating a clear transition from a disordered state to a well-ordered state. For example, in one study azobenzene moieties were grafted to the poly(*n*-butyl methacrylate) block of polystyrene-*block*-poly(*n*-butyl methacrylate) BCPs to cause photoinduced trans−cis isomerization of azobenzene with the goal of inducing order in the BCP.[43] The nonirradiated BCPs showed a single glass transition temperature which would be consistent with phase mixed BCPs. The glass transition temperatures of the irradiated BCPs were not shown, so it is not clear from DSC whether a DOT occurred upon irradiation. X-ray reflectivity indicated that thin films of such BCPs underwent some photoinduced changes, but the morphology could not be precisely determined.

In contrast to the yet explored method of chemical grafting of photoresponsive moieties to impart photoresponsiveness to the block copolymers, here we employ a different and simpler chemistry and governing physics to formulate highly photosensitive disordered block copolymer systems. This strategy relies upon simply blending disordered block copolymers with a photosensitive additive and catalytic amounts of a third ingredient to formulate disordered blends. The MG additive employed in this work was originally designed as stand-alone chemically amplified photoresist and can be efficiently deprotected to yield the −COOH functionality upon UV exposure using PAGs.[34] This photosensitivity is exploited here for the realization of photoinduced ordering to form well-ordered nanoscale features. Thus, the synthetic efforts are significantly minimized because the host BCP does not require grafting of photoresponsive moieties. MGs with similar aromatic cores bearing other protecting groups are also being explored as chemically amplified high-resolution photoresists on account of their small molecular size.[44,45]

A Pluronic triblock copolymer, F127 (EO_{96}−PO_{62}−EO_{96}, ∼12 kg/mol), which has a DOT temperature of approximately 8 °C[46] is chosen as a representative example of a disordered BCP. While the TBCM groups provide weak interaction with F127 ensuring miscibility, the carboxylic acid groups can interact strongly with PEO blocks via hydrogen bonding. Thus, the chemical transformation from MG-TBCM to MG-COOH gives rise to strong interactions that induce ordering of F127 leading to formation of well-ordered morphology.

Differential scanning calorimetry (DSC) measurements were performed to ascertain compatibility of the protected and deprotected forms of the additive in the blends and to compare the interaction of MG-TBCM and MG-COOH with F127. The vertically shifted thermograms are shown in Figure 2. The melting endotherms are ascribed to the melting of PEO crystallites within F127, as PPO does not crystallize. Also shown are the values of the melting temperatures as represented by the endotherm peak positions and the melting enthalpy normalized to the amount of PEO present in the blend. The addition of a strong acid, *p*-toluenesulfonic acid (PTSA) or MG-TBCM, to F127 caused the melting point and melting enthalpy to decrease indicating the compatibility of both PTSA and MG-TBCM with F127. When both PTSA and MG-TBCM were added simultaneously, which results in deprotection of MG-TCBM, PEO crystallization was completely inhibited. This is attributed to the strong interaction of MG-COOH with PEO chains of F127 via hydrogen bonding. Thus, the compatibility of F127 with the additive in both protected and deprotected forms was verified. Further, when these blends were drop casted from their respective solutions on glass slides at 80 °C, which is the temperature at which photoinduced ordering experiments were conducted (discussed later) and is above the melting point of PEO crystallites, all the blends were found to be clear, which indicates formation of homogeneous blends without macrophase separation.

We first employed small-angle X-ray scattering (SAXS) to study the phase behavior of blends F127 with the additive 5,5′-carbonylbis(trimellitic acid) (CTMA), which is similar in functionality to the molecular glass in its deprotected form, MG-COOH. Figure 3 shows that the incorporation of CTMA in F127 induces a DOT. The SAXS profile of neat F127 at 80 °C shows a broad peak, which is a typical signature of disordered BCPs arising due to correlation hole effects or compositional fluctuations.[47,48] However, as CTMA can hydrogen bond with the PEO blocks of F127, incorporation of 30% CTMA causes its ordering as indicated by the sharpening of first peak and appearance of multiple higher order peaks, the positions of which indicate formation of cylindrical morphology (peak position ratios 1, $\sqrt{3}$, $\sqrt{4}$, $\sqrt{7}$). It is also of interest to note the effect of strong interactions on the morphology at 22 °C, which is below

dx.doi.org/10.1021/nl104080v |*Nano Lett.* 2011, 11, 1153–1160

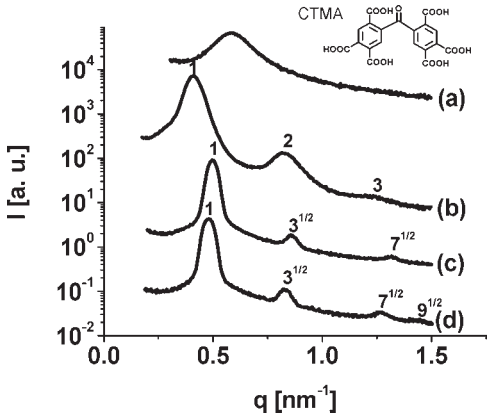

Figure 3. SAXS profiles of (a) neat F127 at 80 °C, (b) neat F127 at 22 °C, (c) 30/70 blend of CTMA/F127 at 80 °C, and (d) 30/70 blend of CTMA/F127 at 22 °C.

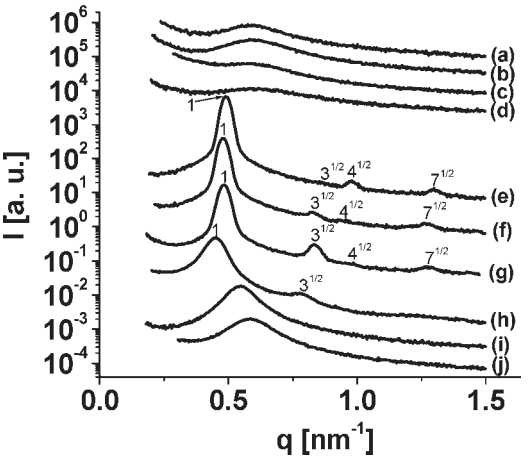

Figure 4. SAXS profiles of neat F127 and its blends with PTSA and/or MG-TBCM at varying compositions at 80 °C: (a) 20/80 MG-TBCM/F127; (b) 30/70 MG-TBCM/F127; (c) 40/60 MG-TBCM/F127; (d) 50/50 MG-TBCM/F127; (e) 20/80/5 MG-TBCM/F127/PTSA; (f) 30/70/5 MG-TBCM/F127/PTSA; (g) 40/60/5 MG-TBCM/F127/PTSA; (h) 50/50/5 MG-TBCM/F127/PTSA; (i) 5/95 PTSA/F127; (j) neat F127. A ratio of higher order peak positions with that of primary peaks indicates hexagonally packed cylindrical morphology for samples that contained both MG-TBCM and PTSA (curves e, f, g, and h).

the melting temperature of PEO crystallites. The SAXS profiles obtained after maintaining the samples at room temperature for 24 h are also shown in Figure 3. Neat F127 shows lamellar morphology (peak position ratios 1, 2, 3, ...) which is not due to an ordered BCP morphology but rather is due to crystallization of PEO below its melting point of 56 °C.[49] In comparison, the room temperature SAXS profile of F127 loaded with 30% CTMA did not show evidence of PEO crystallization and the BCP morphology was maintained upon cooling. Thus, strong interaction of the PEO chains with CTMA inhibits crystallization of PEO and sustains the block copolymer morphology. The behavior of the blend of CTMA with F127 provides an indication of the expected phase behavior for the case of blends of F127 with the MG in deprotected form, i.e., MG-COOH.

Next, we compare the phase behavior of blends of F127 and MG-TBCM with and without the addition of PTSA in Figure 4. The blend composition was varied between 20% MG-TBCM and 50% MG-TBCM. The MG-TBCM in the samples to which PTSA is added deprotects to form MG-COOH. At a range of composition between 20% and 40% MG-TBCM, the blends containing no PTSA were found to be disordered while the blends containing PTSA showed well-defined primary peaks with multiple higher orders of reflection. The results indicate formation of a well-ordered hexagonally packed cylindrical morphology with an interplanar spacing ($d = 2\pi/q^*$) of about 13.0 nm. However, at 50% loading of MG-TBCM with PTSA, the primary peak of the scattering profile broadened, which indicates a loss of a well-ordered structure. The full width at half-maximum intensity (fwhm) for the scattering profiles of neat F127 (fwhm = 0.18) and F127/PTSA blend (fwhm = 0.12) were estimated as discussed previously.[33] While the correlation hole peak for the F127/PTSA blend exhibits a fwmh that is slightly narrower than that of neat F127, it is apparent that the F127/PTSA blend remains phase mixed indicating weak interaction between F127 and PTSA. Likewise, the disordered state of MG-TBCM/F127 blends indicates weak interaction. Thus the ordering of F127 in the presence of the deprotected additive was a result of hydrogen bonding interactions between the carboxylic acid groups of MG-COOH and PEO chains rather than simply due to interaction of PTSA with PEO.

The SAXS and DSC measurements described above confirm that a DOT can be induced in F127 by transitioning from weak to strong interactions between the additive and the BCP. With the governing chemistry and physics in place, the formulation of the BCP system that undergoes photoinduced ordering follows a simple switch of the strong acid PTSA with a PAG, triphenylsulfonium triflate (TPST). Photoinduced ordering experiments were carried out on spin coated films, and scanning force microscopy (SFM) was used to characterize the resulting morphology. The 40% MG-TBCM blend was chosen as the system to demonstrate photoinduced ordering, as this system in deprotected form shows formation of well-ordered morphology and complete inhibition of PEO crystallization. Films of F127 with 40% MG-TBCM and 5 wt % TPST were spin coated onto cleaned Si wafers. As explained in detail in the sample preparation section, the films were baked at 80 °C for 3 min, during which a portion was exposed to UV light (254 nm wavelength) for 1 min to cause liberation of a strong photoacid, which deprotects MG-TBCM to MG-COOH. The solvents employed and the cleaved leaving group byproducts are volatile and leave the films upon spin coating and baking, leaving behind F127, MG-COOH, and the generated acid in the exposed regions. From our previous work it is known that the photoacid[19−21] and additives similar to MG-COOH[33] are selective for the PEO phase as depicted in Figure 1. High loadings of the additives bearing hydrogen bond donating groups are possible due to strong interactions between additive and the PEO chain segments, which are hydrogen bond acceptors.[33] Figure 5 shows representative SFM images of unexposed and exposed regions. The roughness of the film observed in the unexposed region is attributed to crystallization of PEO. The regions that were exposed to UV light showed a fingerprint pattern which indicates formation of well-ordered cylindrical morphology. Since both height and phase images reveal the morphology, it is clear that the photoinduced ordering process caused formation of both topographical and chemical patterns. Additionally, the exposed regions did not show any signs of PEO crystallization, which agrees with the findings in Figure 3 where the crystallization of PEO was found to be inhibited due to strong

dx.doi.org/10.1021/nl104080v |*Nano Lett.* 2011, 11, 1153–1160

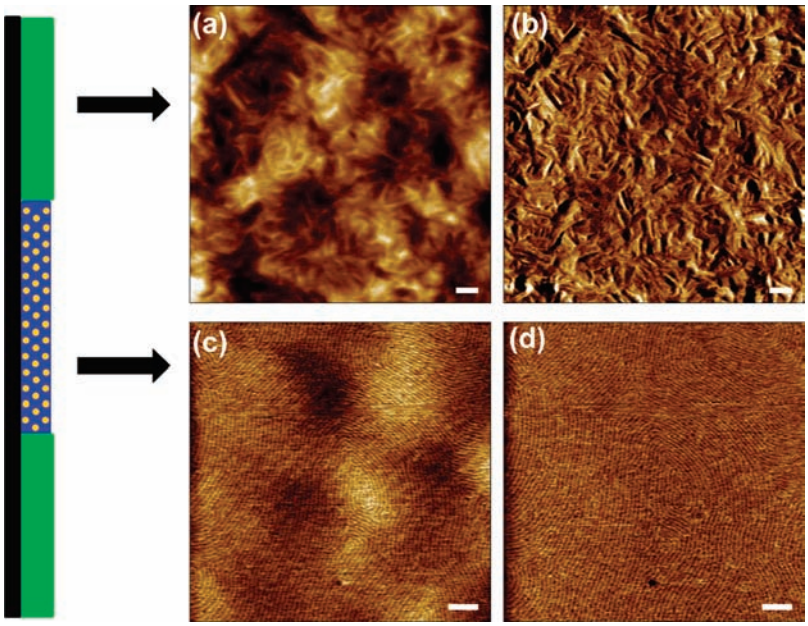

Figure 5. SFM images of unexposed and exposed regions of the film: (a) height image of the unexposed region (z range = 10 nm); (b) phase image of the unexposed region (z range = 22°); (c) height image of the exposed region (z range = 4 nm); (d) phase image of the exposed region (z range = 9°). Unexposed regions are rough due to formation of PEO crystallites while the exposed regions form well-ordered cylindrical morphology showing features in height and phase images thus indicating formation of chemical and topographical BCP pattern. Scale bars = 150 nm.

interactions with carboxylic acid groups. The Supporting Information shows the thicknesses of protected and deprotected films and confirms complete deprotection of MG-TBCM throughout the thickness of the film in the exposed regions. While the films shown in Figure 5 exhibit thicknesses that are greater than a single domain spacing, the concept can be extended to single-domain thickness masks. We recently demonstrated that single-domain thickness masks with cylindrical morphologies and high etch selectivity can be prepared by blending F127 with multiring aromatic additives bearing multiple phenol groups at their periphery. The phenol groups serve as hydrogen bond donors and drive assembly through interactions with the ether oxygen of the PEO segments in a similar manner as the deprotected molecular glass additives described here.[50] Photoinduced ordering in single and multidomain thickness films could further be combined with the existing techniques that allow precise control over the orientational and translational placement of the BCP domains over large areas to realize long-range order in the exposed regions of the films.[1,2] However, for certain applications, for example, fabrication of mesoporous materials using the BCP film as a template, thick films are required and the BCP template does not necessarily require long-range order.[19] One undesirable aspect of the present system as employed here is the roughness in the unexposed regions of the film, which could be an issue for some thin film applications. There are several alternative approaches. These include reversing the volume fractions in the current block copolymer such that PEO is the minor component and PEO crystallization is confined or using films of smaller thicknesses, equivalent to a single domain or a few layers, to limit the volume of PEO crystallization. Ultimately, one could also apply the concepts described here to systems in which the hydrogen bond acceptor block is amorphous.

One additional advantage of this approach over the method of chemical grafting of photoresponsive moieties on block copolymer chains is that the wavelength of UV light can be selected for the PAG employed. Therefore, simply by employing PAGs that can be activated to generate photoacid at different wavelengths, an array of materials that order when exposed to different wavelengths of light could be formulated with the same material. Also, since the intensity of light governs liberation of photoacid from PAGs, generation of 3D microstructures containing ordered domains within an otherwise disordered film could be envisioned by performing a controlled three-dimensional (3D) exposure through 3D fabrication techniques such as holographic lithography.[51,52] The use of an ordered underlying BCP film as a pattern for manipulating the structure of a BCP film on top as demonstrated by Nealey and co-workers[5] could also benefit from this photoinduced ordering strategy because the order in the underlying layer—and consequently the alignment and ordering in the top layer—could now be directed only in regions desired merely by exposing the bilayer films to UV and moderate heating, thus providing a lever to control regions where the top film is modified.

Although F127 was chosen as the disordered BCP, this design of a photoinduced ordering system depends upon the hydrogen bonding interaction of PEO blocks with the additive and therefore it is likely that this strategy could be extended to other PEO containing BCPs as well as to BCPs containing other hydrogen-bonding blocks. For example, as shown in Supporting Figure S1(Supporting Information), in the presence of PTSA, MG-TBCM was found to cause DOT of various other PEO containing BCPs. This additive driven approach is particularly advantageous toward enabling easy scale up because the BCPs themselves do not require any special synthetic procedures to enable photosensitivity. Thus, the ability to independently synthesize the additives and independently choose a relevant BCP and a PAG simplifies the design and yet adds versatility toward the design of BCP systems that undergo photoinduced ordering to form various morphologies when exposed to UV

dx.doi.org/10.1021/nl104080v |*Nano Lett.* 2011, 11, 1153–1160

light of a desired wavelength. We are currently extending this strategy to define submicrometer and nanoscale patterned regions of ordered structures, which are of interest for current and future block copolymer device applications.

Experimental Section. *Materials.* Pluronic triblock copolymer F127 (PEO_{96}−PPO_{62}−PEO_{96}, ∼12 kg/mol) was donated by BASF and *p*-toluenesulfonic acid (PTSA) was obtained from Acros Chemicals. Triphenylsulfonium triflate (TPST), 5,5′-carbonylbis(trimellitic acid) (CTMA), 4-hydroxybenzaldehyde, resorcinol, and *tert*-butyl bromoacetate were purchased from Sigma-Aldrich and used without further purification. *N*,*N*-Dimethylformamide, ethanol, and ethyl acetate were purchased from Sigma-Aldrich and used without further drying.

Synthetic Procedure for MG-TBCM. The synthesis of MG-TBCM follows a two-step procedure as depicted in Supporting Figure S2 (Supporting Information). First MG bearing phenol groups (MG-OH) is synthesized and then the phenol groups are protected with TBCM groups resulting in the formation of protected MG which is denoted as MG-TBCM. MG-OH was synthesized by reacting 4-hydroxybenzaldehyde and resorcinol as done previously by Ober and co-workers[53] based on the condensation reaction of aldehyde and phenols to form MGs also studied by Weinelt and Schneider.[54] The protection of MG-OH with TBCM groups was carried out on lines similar to that employed by Ishii and co-workers:[34] to a magnetically stirred solution of MG-OH (2.44 g, 2.85 mmol) in *N*,*N*-dimethylformamide (DMF, 50 cm^3) K_2CO_3 (9.28 g, 67.1 mmol) and 18-Crown-6 (0.17 g, 0.64 mmol) were added. The suspension was then allowed to equilibrate at 75 °C for 15 min under a N_2 atmosphere. *tert*-Butyl bromoacetate (9.84 g, 50.4 mmol) was then added dropwise to the mixture over 5 min. After the suspension was stirred for 40 h at 75 °C, it was allowed to cool to ambient temperature and concentrated under reduced pressure. The crude product was precipitated during the addition of a citric acid aqueous solution (1 M, 200 cm^3). The solid was filtered, washed with copious amounts of water, redissolved in *N*,*N*-dimethylformamide, and precipitated again from water. The resulting MG-TBCM was dried under reduced pressure to give a brown solid (5.6 g) in which ca. 90% of the phenol groups were converted to TBCM groups, ^{1}H NMR (400 MHz, $CDCl_3$): δ = 1.33−1.58 [m, 98 H, $C(CH_3)_3$], 4.03−4.56 (m, 22 H, $ArOCH_2$), 5.82−6.76 ppm (m, 28 H, Ar−H). The remaining 10% phenol groups promote miscibility of the protected MG with F127 and are therefore advantageous.

Sample Preparation for Small-Angle X-ray Scattering and for Differential Scanning Calorimetry. Samples of neat F127 and its blend with CTMA were made by dissolving their appropriate amounts in DMF by heating at 60 °C with occasional stirring. These solutions were vacuum-dried on glass slides for 2 days in a vacuum oven set at 75 °C.

Samples of neat F127 and its blends with MG-TBCM and/or PTSA were made by dissolving the solids into a cosolvent containing ethanol and ethyl acetate in weight ratio of 1:1. These solutions were kept on a hot plate for 24 h at 75 °C and then drop casted on glass slides kept on a hot plate at 80 °C. The glass slides were kept on the hot plate for about 5 h to ensure complete deprotection after which they were vacuum-dried at 70 °C for 1 day.

Binary blend compositions are reported as weight ratio of additive to F127. For example, a blend referred to as 30/70 contains 30% additive and 70% F127. For ternary blends to which MG-TBCM, F127, and PTSA or TPST were added, blend compositions are represented as $x/y/z$. Here, x and y denote the ratio of MG-TBCM and F127 and $z/100$ denotes the amount of PTSA or TPST added per gram of the MG-TBCM/F127 blend. For example, a 40/60/5 blend of MG-TBCM, F127 and PTSA implies a 40/60 blend of MG-TBCM and F127 to which 0.05 g of PTSA was added per gram of the 40/60 blend.

Small Angle X-ray Scattering. For SAXS, the dried samples were placed in the center of 1 mm thick metal washers and sealed on both sides with Kapton film. The filled metal washers were put in metal cells that fit on a vertical heater installed inside the sample chamber and equilibrated at 80 °C for about 30 min. For measurements done at 22 °C (room temperature), the same samples were kept at room temperature for 24 h before measurements. SAXS was performed using an instrument from Molecular Metrology, Inc. (presently sold as Rigaku S-Max3000). It impinges a 0.4 mm diameter X-ray beam of wavelength 0.1542 nm produced by a copper source. The whole system is evacuated during operation and allows measurements in wave vector (q) range of $0.06 < q < 1.6$ nm^{-1} in which $q = (4\pi/\lambda) \sin\theta$, where 2θ is the scattering angle. The sample to detector distance was calibrated using silver behenate standard peak at 1.076 nm^{-1}. A two-dimensional gas-filled wire detector was used for collection of scattered X-ray. The raw scattering data were circularly averaged and plotted as intensity vs q where intensity was used in arbitrary units as the profiles obtained were shifted vertically to avoid overlap.

Differential Scanning Calorimetry. The samples prepared for SAXS were also used for DSC to obtain complementary data. Sample masses of 12−18 mg were filled into aluminum pans, hermetically sealed, kept at 80 °C in an oven, and removed one at a time for measurement. DSC thermograms were measured using a TA Instruments Q100 DSC equipped with an RCS cooling system and nitrogen gas purge with a flow rate of 50 mL/min. Temperature calibration was carried out using indium as a standard (T_m = 156.6 °C) and the indium heat of fusion (28.6 J/g) was used to calibrate the heat flow. All measurements were conducted in the temperature range of −90 to 80 °C at a constant heating and cooling rate of 10 °C/min under nitrogen atmosphere. The DSC thermograms obtained between 15 and 80 °C during the second heating cycle are reported. The melting temperature and melting enthalpy were estimated using Universal Analysis software from TA Instruments. The estimated melting enthalpies were normalized with respect to the weight of PEO in the blend.

Sample Preparation for Scanning Force Microscopy. For spin coating thin films for photoinduced ordering and SFM characterization, solutions (5 wt % solids) of MG-TBCM with F127 and TPST were made by dissolving appropriate amounts of solids into ethanol−ethyl acetate (1:1 by weight) cosolvent. These solutions were kept on a hot plate at 60 °C for 2 h to dissolve the contents. The solutions were filtered through 0.2 μm PTFE filters and spin coated at 2000 rpm on silicon wafers cleaned with carbon dioxide snowjet followed by an oxygen plasma treatment. The spin coated films were placed immediately on a hot plate set at 80 °C kept underneath a 254 nm wavelength UV lamp and some portions of the films were covered by aluminum foil to mask off exposure to UV light. The films were kept on the hot plate for a total of 3 min, and the UV lamp was switched on to expose the unmasked portion of the film to UV light in the middle one minute of the 3 min heating cycle. At the end of 3 min the wafers were removed from the hot plate and the exposed and unexposed regions were characterized at room temperature by SFM.

Scanning Force Microscopy. SFM was carried out on a Veeco Dimension 3100 scope with a Nanoscope III controller operated in tapping mode to acquire the phase and height images.

■ ASSOCIATED CONTENT

Supporting Information. Additional information on occurrence of ordering of other PEO containing BCPs when the blended MG-TBCM is converted to MG-COOH, synthesis scheme for MG-TBCM, and thickness of exposed and unexposed films obtained by spectroscopic ellipsometry. This material is available free of charge via the Internet at http://pubs.acs.org.

■ AUTHOR INFORMATION

Corresponding Author

*E-mail: watkins@polysci.umass.edu.

Present Addresses

[||]Department of Polymer Science and Engineering, Inha University, Incheon 402-751, South Korea.

■ ACKNOWLEDGMENT

This work was supported by the NSF Center for Hierarchical Manufacturing at the University of Massachusetts (CMMI-0531171). E.L.S. would like to acknowledge the Semiconductor Research Corporation for funding.

■ REFERENCES

(1) Albert, J. N. L.; Epps, T. H. *Mater. Today* **2010**, *13* (6), 24–33.
(2) Marencic, A. P.; Register, R. A. Controlling Order in Block Copolymer Thin Films for Nanopatterning Applications. *Annu. Rev. Chem. Biomol. Eng.* **2010**, *1*, 277–297.
(3) Ruiz, R.; Kang, H. M.; Detcheverry, F. A.; Dobisz, E.; Kercher, D. S.; Albrecht, T. R.; de Pablo, J. J.; Nealey, P. F. *Science* **2008**, *321*, 936–939.
(4) Stoykovich, M. P.; Muller, M.; Kim, S. O.; Solak, H. H.; Edwards, E. W.; de Pablo, J. J.; Nealey, P. F. *Science* **2005**, *308*, 1442–1446.
(5) Park, S. M.; Ravindran, P.; La, Y. H.; Craig, G. S. W.; Ferrier, N. J.; Nealey, P. F. *Langmuir* **2007**, *23*, 9037–9045.
(6) Bita, I.; Yang, J. K. W.; Jung, Y. S.; Ross, C. A.; Thomas, E. L.; Berggren, K. K. *Science* **2008**, *321*, 939–943.
(7) Park, S.; Lee, D. H.; Xu, J.; Kim, B.; Hong, S. W.; Jeong, U.; Xu, T.; Russell, T. P. *Science* **2009**, *323*, 1030–1033.
(8) Kim, S. H.; Misner, M. J.; Xu, T.; Kimura, M.; Russell, T. P. *Adv. Mater.* **2004**, *16*, 226–231.
(9) Kim, G.; Libera, M. *Macromolecules* **1998**, *31*, 2569–2577.
(10) Kimura, M.; Misner, M. J.; Xu, T.; Kim, S. H.; Russell, T. P. *Langmuir* **2003**, *19*, 9910–9913.
(11) Park, S.; Kim, B.; Xu, J.; Hofmann, T.; Ocko, B. M.; Russell, T. P. *Macromolecules* **2009**, *42*, 1278–1284.
(12) Han, E.; Stuen, K. O.; La, Y. H.; Nealey, P. F.; Gopalan, P. *Macromolecules* **2008**, *41*, 9090–9097.
(13) Morkved, T. L.; Lu, M.; Urbas, A. M.; Ehrichs, E. E.; Jaeger, H. M.; Mansky, P.; Russell, T. P. *Science* **1996**, *273*, 931–933.
(14) Park, M.; Harrison, C.; Chaikin, P. M.; Register, R. A.; Adamson, D. H. *Science* **1997**, *276*, 1401–1404.
(15) Stoykovich, M. P.; Nealey, P. F. *Mater. Today* **2006**, *9*, 20–29.
(16) Harrison, C.; Park, M.; Chaikin, P. M.; Register, R. A.; Adamson, D. H. *J. Vac. Sci. Technol., B* **1998**, *16*, 544–552.
(17) Jung, Y. S.; Jung, W.; Tuller, H. L.; Ross, C. A. *Nano Lett.* **2008**, *8*, 3776–3780.
(18) Cheng, J. Y.; Ross, C. A.; Chan, V. Z. H.; Thomas, E. L.; Lammertink, R. G. H.; Vancso, G. J. *Adv. Mater.* **2001**, *13*, 1174–1178.
(19) Pai, R. A.; Humayun, R.; Schulberg, M. T.; Sengupta, A.; Sun, J. N.; Watkins, J. J. *Science* **2004**, *303*, 507–510.
(20) Tirumala, V. R.; Pai, R. A.; Agarwal, S.; Testa, J. J.; Bhatnagar, G.; Romang, A. H.; Chandler, C.; Gorman, B. P.; Jones, R. L.; Lin, E. K.; Watkins, J. J. *Chem. Mater.* **2007**, *19*, 5868–5874.
(21) Nagarajan, S.; Li, M. Q.; Pai, R. A.; Bosworth, J. K.; Busch, P.; Smilgies, D. M.; Ober, C. K.; Russell, T. P.; Watkins, J. J. *Adv. Mater.* **2008**, *20*, 246–251.
(22) Kang, M.; Moon, B. *Macromolecules* **2009**, *42*, 455–458.
(23) Jackson, E. A.; Hillmyer, M. A. *ACS Nano* **2010**, *4*, 3548–3553.
(24) Cui, Y.; Wei, Q. Q.; Park, H. K.; Lieber, C. M. *Science* **2001**, *293*, 1289–1292.
(25) Timko, B. P.; Cohen-Karni, T.; Qing, Q.; Tian, B. Z.; Lieber, C. M. *IEEE Trans. Nanotechnol.* **2010**, *9*, 269–280.
(26) Aydin, D.; Louban, I.; Perschmann, N.; Blummel, J.; Lohmuller, T.; Cavalcanti-Adam, E. A.; Haas, T. L.; Walczak, H.; Kessler, H.; Fiammengo, R.; Spatz, J. P. *Langmuir* **2010**, *26*, 15472–15480.
(27) Bates, F. S.; Fredrickson, G. H. *Phys. Today* **1999**, *52*, 32–38.
(28) Chen, J.; Frisbie, C. D.; Bates, F. S. *J. Phys. Chem. C* **2009**, *113*, 3903–3908.
(29) Epps, T. H.; Bailey, T. S.; Pham, H. D.; Bates, F. S. *Chem. Mater.* **2002**, *14*, 1706–1714.
(30) Kim, S. H.; Misner, M. J.; Yang, L.; Gang, O.; Ocko, B. M.; Russell, T. P. *Macromolecules* **2006**, *39*, 8473–8479.
(31) Tirumala, V. R.; Daga, V.; Bosse, A. W.; Romang, A.; Ilavsky, J.; Lin, E. K.; Watkins, J. J. *Macromolecules* **2008**, *41*, 7978–7985.
(32) Tirumala, V. R.; Romang, A.; Agarwal, S.; Lin, E. K.; Watkins, J. J. *Adv. Mater.* **2008**, *20*, 1603–1608.
(33) Daga, V. K.; Watkins, J. J. *Macromolecules* **2010**, *43*, 9990–9997.
(34) Iimori, H.; Shibasaki, Y.; Ueda, M.; Ishii, H. *J. Photopolym. Sci. Technol.* **2003**, *16*, 685–689.
(35) Rosenhauer, R.; Fischer, T.; Stumpe, J.; Gimenez, R.; Pinol, M.; Serrano, J. L.; Vinuales, A.; Broer, D. *Macromolecules* **2005**, *38*, 2213–2222.
(36) Yu, H. F.; Iyoda, T.; Ikeda, T. *J. Am. Chem. Soc.* **2006**, *128*, 11010–11011.
(37) Morikawa, Y.; Kondo, T.; Nagano, S.; Seki, T. *Chem. Mater.* **2007**, *19*, 1540–1542.
(38) Morikawa, Y.; Nagano, S.; Watanabe, K.; Kamata, K.; Iyoda, T.; Seki, T. *Adv. Mater.* **2006**, *18*, 883–886.
(39) Tran-Cong-Miyata, Q.; Nishigami, S.; Ito, T.; Komatsu, S.; Norisuye, T. *Nat. Mater.* **2004**, *3*, 448–451.
(40) Schumers, J. M.; Fustin, C. A.; Gohy, J. F. *Macromol. Rapid Commun.* **2010**, *31*, 1588–1607.
(41) Zheng, P. J.; Hu, X.; Zhao, X. Y.; Li, L.; Tam, K. C.; Gan, L. H. *Macromol. Rapid Commun.* **2004**, *25*, 678–682.
(42) Zhao, Y.; Thorkelsson, K.; Mastroianni, A. J.; Schilling, T.; Luther, J. M.; Rancatore, B. J.; Matsunaga, K.; Jinnai, H.; Wu, Y.; Poulsen, D.; Frechet, J. M. J.; Alivisatos, A. P.; Xu, T. *Nat. Mater.* **2009**, *8*, 979–985.
(43) Huang, C. F.; Chen, W.; Russell, T. P.; Balazs, A. C.; Chang, F. C.; Matyjaszewski, K. *Macromol. Chem. Phys.* **2009**, *210*, 1484–1492.
(44) Dai, J. Y.; Chang, S. W.; Hamad, A.; Yang, D.; Felix, N.; Ober, C. K. *Chem. Mater.* **2006**, *18*, 3404–3411.
(45) De Silva, A.; Felix, N. M.; Ober, C. K. *Adv. Mater.* **2008**, *20*, 3355–3361.
(46) Patrick, J.; Fairclough, A.; Yu, G. E.; Mai, S. M.; Crothers, M.; Mortensen, K.; Ryan, A. J.; Booth, C. *Phys. Chem. Chem. Phys.* **2000**, *2*, 1503–1507.
(47) Leibler, L. *Macromolecules* **1980**, *13*, 1602–1617.
(48) Zhang, F. J.; Stuhn, B. *Colloid Polym. Sci.* **2006**, *284*, 823–833.
(49) Innocenzi, P.; Malfatti, L.; Piccinini, M.; Marcelli, A. *J. Phys. Chem. A* **2010**, *114*, 304–308.
(50) Chandler, C. M.; Schwartz, E. L.; Daga, V. K.; Ober, C. K.; Watkins, J. J. Submitted to *Chem. Mater.*

(51) Moon, J. H.; Ford, J.; Yang, S. *Polym. Adv. Technol.* **2006**, *17*, 83–93.
(52) Jang, J. H.; Ullal, C. K.; Maldovan, M.; Gorishnyy, T.; Kooi, S.; Koh, C. Y.; Thomas, E. L. *Adv. Funct. Mater.* **2007**, *17*, 3027–3041.
(53) Chang, S. W.; Ayothi, R.; Bratton, D.; Yang, D.; Felix, N.; Cao, H. B.; Deng, H.; Ober, C. K. *J. Mater. Chem.* **2006**, *16*, 1470–1474.
(54) Weinelt, F.; Schneider, H. J. *J. Org. Chem.* **1991**, *56*, 5527–5535.